Surface Plasmon Resonance Sensors for Medical Diagnosis

10

Yeşeren Saylan, Fatma Yılmaz, Erdoğan Özgür, Ali Derazshamshir, Nilay Bereli, Handan Yavuz, and Adil Denizli

Contents

Y. Saylan · A. Derazshamshir · N. Bereli · H. Yavuz · A. Denizli (✉)
Department of Chemistry, Hacettepe University, Ankara, Turkey
e-mail: denizli@hacettepe.edu.tr

F. Yılmaz
Department of Chemistry Technology, Abant Izzet Baysal University, Bolu, Turkey

E. Özgür
Department of Chemistry, Hacettepe University, Ankara, Turkey

Department of Chemistry, Aksaray University, Aksaray, Turkey

C. S. S. R. Kumar (ed.), *Nanotechnology Characterization Tools for Biosensing and Medical Diagnosis*, https://doi.org/10.1007/978-3-662-56333-5_10

1 Definition of the Topic

Surface plasmon resonance (SPR) sensors have fascinated impressive attention to detect clinically related analytes in recent years. SPR sensors have also multiple advantages over existing conventional diagnostic tools such as easy preparation, no requirement of labeling, and high specificity and sensitivity with low cost, and they provide real-time detection capability. There are some articles and reviews in literature focusing on the applications of SPR-based sensors for the diagnosis of medically important entities such as proteins, cells, viruses, disease biomarkers, etc. These articles generally give information about the determination of these structures, whereas this presented manuscript combines recent literature for most of the medically important structures together including proteins, hormones, nucleic acids, whole cells and drugs that especially the latest applications of SPR sensors for medical diagnosis to follow up new strategies and discuss how SPR strategy is brought to solve the medical problems.

2 Overview

A large number of potential analytical difficulties in various fields that can be easily figured out by the tools are called sensors. Medical and health problems have emerged because of the increasing population with a high risk of chronic and infection diseases such as heart disease, stroke, cancer, tuberculosis that need to be solved for public health.

This chapter is structured according to the principle of SPR, the importance of SPR in medical diagnosis, key research findings according to the diagnosis of diseases, and conclusions and future perspective. Latest strategies and novel applications are focused in this chapter by a discussion on how SPR technology is brought to solve the medical problems.

3 Introduction

The detection of clinically relevant molecules such as proteins, hormones, nucleic acids, cells, and drugs is essential to understanding their biological and physiological functions and also to developing medical diagnostics tools. These molecules accomplish many biological functions, including storing and transmitting genetic information, regulating biological activities, transporting molecules, and catalyzing reactions. Moreover, they can be used as biomarkers in the diagnosis of many diseases [1]. Analytical devices, called sensors, consist of a transducer and recognition elements capture a specific analyte for the analysis of a sample mixture to evaluate their composition, structure and function by converting biological responses into electrical signals are called sensors. Regarding the transduction principles, sensors can be classified as optical [2–4], electrochemical [5–7], mass [8–10], magnetic [11–13], and micromechanical [14–16].

Development of optical sensors has been fascinating in the past two decades, due to their immunity to electromagnetic interference and ability to perform remote sensing and to supply multiple detections with one device. Sensors utilize a variety of optical sensing methods that include chemiluminescence, fluorescence, light absorption and scattering, reflectance, and surface plasmon resonance and can be separated into two classes: label-based and label-free.

Industrious labeling methods may hinder with the function of a molecule in spite of label-based detections with the detection limit value down to a single molecule which is extremely sensitive. Quantitative studies are challenging because of the fluorescence signal bias due to the few fluorophores on each molecule, which cannot be correctly controlled. In opposing, binding-induced refractive index changes are measured with the label-free detections [17].

Surface plasmon resonance (SPR) is a very suitable technology to detect clinical analytes for a number of aims. Due to the detection that depends on refractive index changes, specific bindings are quantified as they happen without time-consuming washes of unbounds, and this feature reduces time-to-result compared with other technologies. In addition, the detection does not base on labeling of the target molecules. Because the labeling of a target may alter its binding affinity and kinetics properties and also increase the complexity of the reaction and the cost of the process. Furthermore, SPR is able to detect many clinical analytes directly. It can be used to improve detection sensitivity, selectivity, and/or refractive index resolution. SPR only needs basic optics that can be miniaturized to a size that is suitable for medical diagnosis. Besides, the non-specific interactions with SPR surface in a complex mixture can be reduced by the ability to have multiple reference surfaces that may be used to correct background signals [18].

4 Experimental and Instrumental Methodology

4.1 Principle of Surface Plasmon Resonance

Refractive index changes occur in the very close vicinity of a metal surface of the SPR sensors. This function generally appears between two transparent media and then measured by a simple and direct sensing onto the SPR sensors. Plane-polarized light can undergo total internal refraction when the beam enters into the higher refractive index medium at above its critical angle. Under optimal conditions, electromagnetic field component of the light, which is penetrating into the gold film, is called an evanescent wave. The interaction of this wave with free oscillating electrons at the metal surface will produce the excitation of surface plasmons at a specific angle of incidence and results in a decline of the reflected light intensity subsequently [19].

Utilization of the optical phenomenon, SPR, has seen extensive growth since its initial observation by Wood in the early 1900s [20]. It was initially exploited for a variety of spectroscopic and physical characterizations including enhanced holography [21], surface-enhanced Raman scattering or coherent anti-Stokes Raman scattering, and surface plasmon microscopy for high contrast imaging of thin dielectric

films [22–24]. SPR is a simple and direct sensing technique that can be used to probe refractive index changes that occur in the very close vicinity of a thin metal film surface [25]. This technique utilizes a thin film of metal between two transparent media of different refractive index to function as an optical sensor surface. Above a critical angle, a plane-polarized light beam entering the higher refractive index medium can undergo total internal refraction. Under these conditions, an electromagnetic field component of the light called the evanescent wave will penetrate into the gold film. At a specific angle of incidence, the interaction of this wave with free oscillating electrons at the gold film surface will cause the excitation of surface plasmons, resulting subsequently in a decrease in the reflected light intensity. This phenomenon is called surface plasmon resonance and occurs only at a specific angle known as the resonant angle. This SPR angle is modified by the addition of the analyte onto the gold film surface, thereby allowing the monitoring of binding events. From a practical standpoint, the Kretschmann prism arrangement is the most frequently employed geometry in SPR.

An estimation of the penetration depth is given by the following expressions [26]:

$$d_{\mathrm{p}} = \frac{\lambda}{4\pi\sqrt{\eta_1^2 \sin^2\theta - \eta_2^2}} \tag{10.1}$$

where η_1 and η_2 are the refractive index of medium 1 and medium 2, respectively. Typically, this will be approximately equal to one-fourth of the incident light wavelength.

The light that is p-polarized with respect to the metal surface is launched into the prism for coupling to the metal film only p-polarized light can be utilized for plasmon generation because this particular polarization has the electric field vector oscillations normal to the metal film. This is referred to as the transverse magnetic wave of the electron plasma along the flat metal surface [27, 28]. In contrast, the s-polarized transverse electric polarization cannot generate surface plasmons since its electric field vector is orientated parallel to the metal film. The wave vector of the oscillations, K_{sp}, is given by the expression:

$$K_{\mathrm{sp}} = \frac{\omega}{c}\sqrt{\frac{\varepsilon_{\mathrm{m}}\varepsilon_{\mathrm{s}}}{\varepsilon_{\mathrm{m}} + \varepsilon_{\mathrm{s}}}} \tag{10.2}$$

where ω is the frequency of the oscillations, c is the speed of light, ε_{s} is the dielectric function of the sample medium adjacent to the metal surface, and ε_{m} is the dielectric function of the metal. The wave vector for a component of incident light can be described by the equation:

$$K_{\mathrm{x}} = \frac{\omega}{c}\eta \sin\theta \tag{10.3}$$

where θ is the angle of incidence of the light onto the metal film and η the refractive index of the prism. Surface plasmons, which oscillate and propagate along the upper

surface of the metal film, absorb some of the p-polarized light energy from the evanescent field to change the total-internal-reflection light intensity Ir. Therefore, a plot of Ir versus incidence (or reflection) angle (θr) produces an angular intensity profile that exhibits a sharp dip at the resonance angle.

The surface plasmon wave vector can be related to the refractive index of the medium on the near vicinity of the metal film by simplification of the equation. Disregarding the imaginary portion of ε, K_{sp} can be rewritten as:

$$K_{sp} = \frac{\omega}{c}\sqrt{\frac{\eta_m^2 \eta_s^2}{\eta_m^2 + \eta_s^2}} \tag{10.4}$$

where η_m is the refractive index of the metal and η_s is the refractive index of the sample. The imaginary component of the complex refractive index term can be related to absorbance.

4.2 Importance of SPR in the Medical Diagnosis

SPR technology first emerged many years ago, and then many scientists that include chemists, biologists, physicists, and medical doctors have joined to use the SPR as a novel application in various fields, such as doping analysis [29], diagnosis [30], food safety [31], laboratory medicine [32], etc. Among them, definitely, clinical studies have also been investigated as an effective application area. Superior features of the SPR technology enable several advantages involving detecting of the target molecules in real-time, label-free analysis, need low sample amount, quantitative reply, and high sensitivity and reusability. These features make SPR technology desirable for point-of-care diagnostics that can do fast and multi-analyte detection [33]. In this chapter, the key research findings that include protein, hormone, nucleic acid, cell, and drug detection for several diseases were summarized according to the latest literature.

5 Key Research Findings

5.1 Protein Detection

Clinically relevant proteins which have very important features to diagnose the level of related diseases are needed trusty methods to detect them in complex mixtures. Detection of proteins leads to molecularly targeted therapy and also measures a therapeutic reaction. The SPR sensors supply an applicable system for clinical analysis [34, 35]. The most recent studies based on SPR sensor to detect proteins for a number of diseases were focused in this part.

There are too many different cancer types associated with deregulated genes and signaling pathways. Successful diagnosis of early stage cancer and follow-up

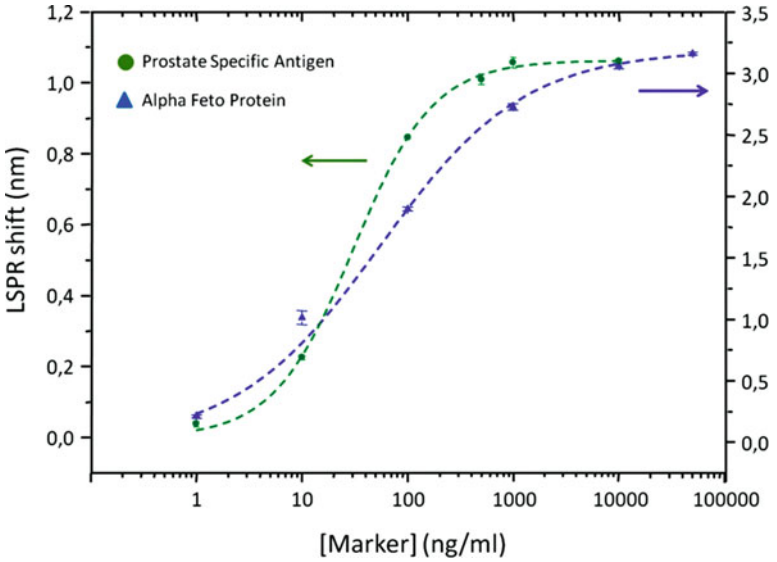

Fig. 10.1 Parallel sensor response for the detection of alpha-fetoprotein and prostate-specific antigen cancer markers [38]

treatment is vital for cancer biomarkers detection. SPR sensors offer a promising platform for rapidly target analysis, which can be used for cancer diagnosis, prognosis, and drug monitoring. They have lately performed for molecular signature profiling, dynamic functional analysis, tumor cell enrichment and purification [36]. The art of synthesizing SPR-based sensing materials has largely been improved by the recent advancements in the area of functional nanomaterials and has offered tunable surface plasmon characteristics meant for specific purposes. The trend for the use of label-free and reusable functionalized nanomaterials has greatly improved sensing capabilities of different cancer biomarkers, and the doors have been widely opened to design multiplexed analysis platforms [37].

Eight microfluidic channels based thirty-two sensing sites for monitoring cancer biomarker such as a prostate specific antigen and human alpha-fetoprotein up to a concentration of 500 pg/mL was designed by Aćimović and collaborators [38]. As seen in Fig. 10.1, they first considered alpha-fetoprotein (blue curve) and observed small fluctuations in concentration of alpha-fetoprotein in human serum below the clinically significant level. To detect alternative markers, they demonstrated (green curve) whole detection of prostate-specific antigen to show quick sensing platform for detection of analyte in the ng/mL concentration range in a matter of minutes with outstanding reproducibility.

The detection of prostate-specific antigen was also performed with UV polymerization method based on the micro-contact imprinting technique by prostate-specific antigen-imprinted SPR sensor [39]. They performed the prostate-specific antigen detection with standard prostate-specific antigen solutions in a concentration range

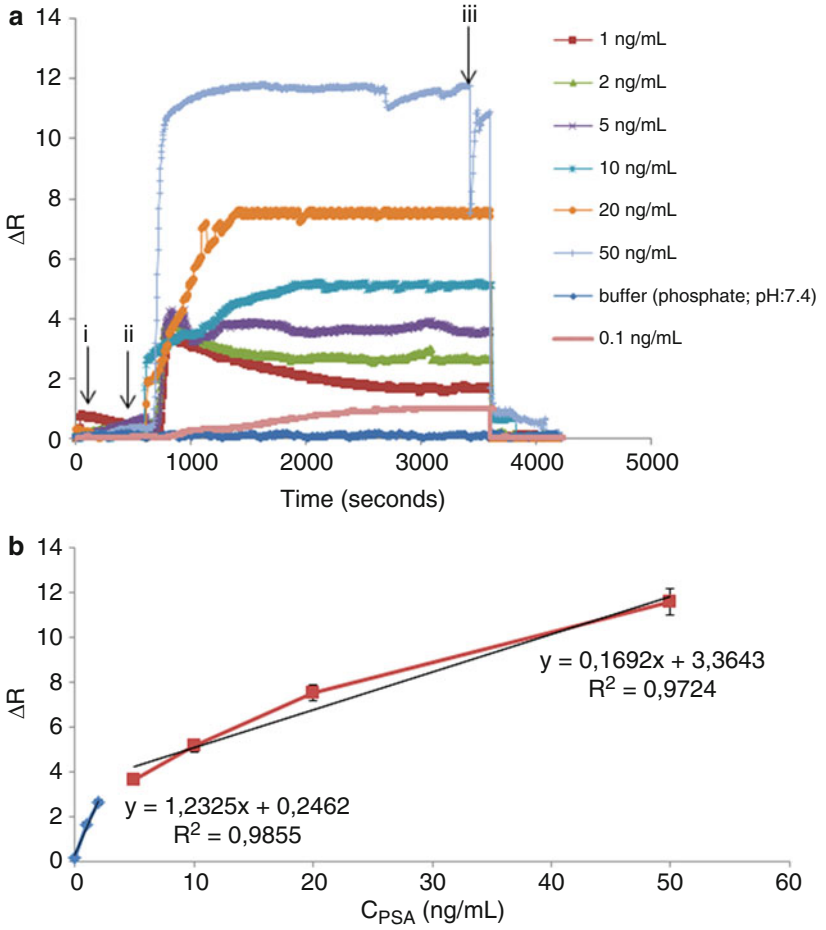

Fig. 10.2 (**a**) The prostate-specific antigen detection, (**b**) calibration curve for prostate-specific antigen detection measured with the SPR sensor [39]

of 0.1–50 ng/mL and found the limit of detection (LOD) value as 91 pg/mL. As seen in Fig. 10.2a, they equilibrated with phosphate buffer (i), injected with the analyte solutions (ii), and desorbed with glycine – HCl (iii). They also obtained high correlation coefficients after performing different samples (Fig. 10.2b). They applied ten clinical serum samples to the SPR sensor and obtained the results; 98% agreement with ELISA method without important differences at the 0.05 level was indicated.

Point-of-care diagnostic sensor for total prostate-specific antigen detection in human serum samples using SPR sensor platforms was developed by Uludag et al. [40]. They used a sandwich assay on an SPR sensor based on antibody-modified nanoparticles to detect the different concentration of total prostate-specific antigen in human serum. They calculated K_D value as 9.46×10^{-10} M, designating an excellent affinity of the antibody employed in their assay. They showed that the

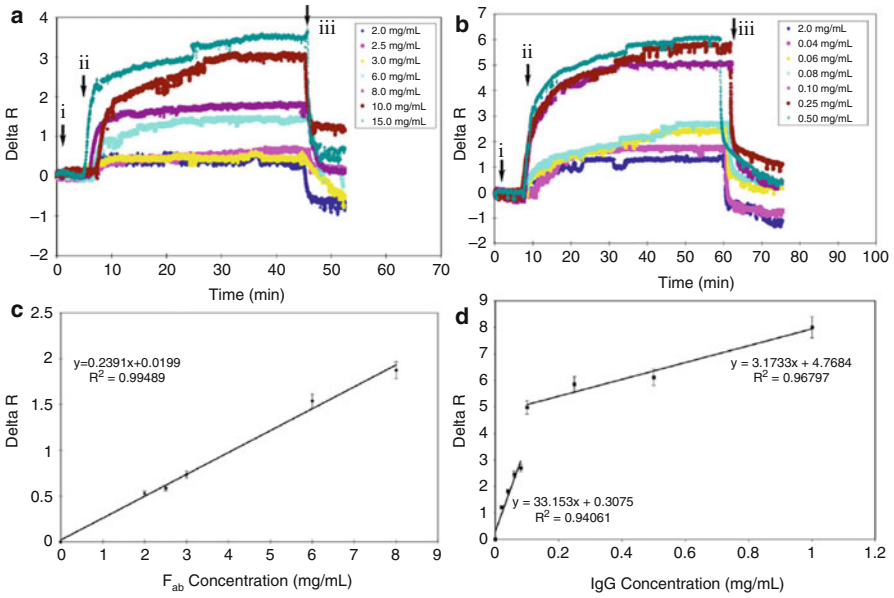

Fig. 10.3 The (**a**) F_{ab}, (**b**) IgG detection, reflectivity vs (**c**) F_{ab}, and (**d**) IgG concentration dependency of the SPR chip response [42]

developed immunoassay-based SPR sensor could be successfully utilized to patient's serum samples as clinical application.

Immunoglobulins (Ig) used in in vivo diagnostics have gained significant notice among health authorities over the world. For this purpose, detection of human IgG in human serum by polymeric nanoparticles fixed to SPR sensor was indicated by Türkoğlu and collaborators [41]. They also performed kinetic studies by using IgG samples with different concentration (0.05–2.0 mg/mL). They observed that the reflectivity value was increased from 0.3 to 2.5 in parallel to IgG concentration that increased from 0.05 to 2.0 mg/mL when the IgG samples were applied.

Ertürk and coworkers prepared F_{ab} fragments imprinted SPR sensor to detect human IgG [42]. F_{ab} fragments were digested with papain and collected by fast protein liquid chromatography system, and then collected F_{ab} fragments reacted with the specific monomer (N-methacryloyl-l-histidine methyl ester) to prepare nanofilm on SPR sensor surface in the existence of cross-linker (ethylene glycol dimethacrylate) and functional monomer (2-hydroxyethylmethacrylate). IgG detection studies were carried out by using a different concentration of aqueous IgG solutions. They also performed selectivity experiments of the F_{ab} imprinted SPR sensor by employing bovine serum albumin (BSA), IgG, and F_{ab} and F_c fragments in singular and multiple mixtures (Fig. 10.3). According to their results, they found the LOD value as 56 ng/mL.

Rheumatoid arthritis identified with common chronic joint inflammation is an autoimmune disease. The anti-cyclic citrullinated peptide is IgG antibodies which

act as a significant role in the diagnosis of this disease. Dibekkaya et al. prepared anti-cyclic citrullinated peptide imprinted SPR sensor to detect cyclic citrullinated peptide antibodies [43]. They examined the selectivity experiments by utilizing IgM and BSA. They calculated maximum reflection, LOD, association (K_a), and dissociation (K_d) constants as 1.079 RU/mL, 0.177 RU/mL, 0.589 RU/mL, and 1.697 mL/RU, respectively.

Hepatitis B virus infection is still an important global problem. The feasibility of SPR sensor was tested by Chung and collaborators to the diagnosis of human hepatitis B virus antibodies [44]. They optimized the baseline stability and the dilution factor of serum samples for SPR sensor application with phosphate buffer saline and 0.5% Tween 20 solution. They estimated the baseline stability as 69.79° with a standard deviation of 0.32 millidegree. They calculated that SPR change of 120 millidegree equaled to protein binding of 1 ng/mm^2. Samples of hepatitis B virus antibodies were used to prepare a standard curve. They used secondary antibodies to test the sensitivity of the SPR sensor. They claimed that the LOD value of the SPR sensor for the medical diagnosis was very similar to the ELISA kit for the diagnosis of hepatitis.

Diagnosis of hepatitis B surface antibody in human serum by hepatitis B surface antibody imprinted polymeric film, which was attached to the SPR sensor, was prepared by Uzun et al. [45]. They performed kinetic studies using the hepatitis B surface antibody-positive human serum. They found the LOD value as 208.2 mIU/mL. Nonimmunized, hepatitis B surface antibody-negative serum was used for performing control experiments of the SPR sensor. Results obtained by control experiments showed that SPR sensor did not give any noticeable response to hepatitis B surface antibody-negative serum.

Inflammatory bowel disease patients are treated with therapeutic monoclonal antibody, infliximab, and therapeutic outcomes are monitored infliximab trough concentrations. Lu et al. reported an assay by employing an in-house fiber-optic SPR sensor for the infliximab determination in serum [46]. They observed that SPR response was increased by using gold nanoparticles functionalized with another set of infliximab-specific antibodies. They obtained the calibration curves with a series of infliximab concentrations spiked in the buffer and serum with the LOD values of 0.3 and 2.2 ng/mL, consequently. They claimed that their results were compared with ELISA resulting in outstanding Pearson and intraclass correlation coefficients of 0.998 and 0.983.

Immobilization of a human growth hormone on the self-assembled monolayer-based SPR sensor for specific antihuman growth hormone antibodies detection using the combination of three different physical phenomena in the same channel of the SPR was performed by Ramanaviciene et al. [47]. Detection of the specific antihuman growth hormone antibodies using secondary assay format on the same domain of the SPR sensor was shown successfully by simultaneous exploitation of several techniques. They performed the secondary antibody binding to the immune complex formed between the immobilized human growth hormone and different concentrations of antihuman growth hormone (from 0.098 to 39.47 nM) at pH 7.4 by SPR study. Finally, they calculated LOD value as 0.051 nM for SPR system.

Exosomes that have the suitable features for cancer diagnostics such as molecular contents of the movement of the cell, which they create in spite of the exosomes detection, are technically contesting. Quantitative analyses of exosomes by an approach were described by Im and coworkers [48]. They functionalized the nanoholes with antibodies for a description of the exosome surface and lysate proteins to produce nanoplasmonic exosome assay, which was based on transmission SPR. They examined exosome-binding kinetics and calculated the constants K_a, K_d, and k_D as 1.6×10^7 M^{-1} s^{-1}, 4.8×10^{-4} s^{-1}, and 3.6×10^{-11} M, respectively. They observed binding constant as approximately 36 pM and claimed that this value was lower than that of individual antigen-antibody binding (1 nM). They improved the sensitivity by this approach to operating when integrated with miniaturized optics and retrieval of exosomes. They found that exosomes having the potential for diagnostics originated from ovarian cancer cells could be specified by their expression of CD24 and EpCAM by analyzing ascites samples from ovarian cancer.

The other study which described the growth of a sensor to detect folic acid protein using graphene-based SPR sensor was described by He and coworkers [49]. The exceptional properties of graphene were exploited to construct the SPR sensor for folate biomarker sensing in serum. The specific recognition of folic acid protein is based on the interactions between folic acid receptors integrated through π-stacking on the graphene-coated SPR sensor and the folic acid protein analyte in serum. Sensing capabilities for folate biomarkers were kept by a simple post-adsorption of human serum and bovine serum albumin mixtures onto the folic acid-modified sensor resulting in a highly antifouling interface. They examined the different concentration of folic acid (10 fM–1 pM) and declared that sensor allowed fM detection of folic acid protein, a detection limit well adapted and promising for quantitative clinical analysis.

Amplification technique by using magnetic nanoparticles with core-shell structure for an SPR sensor was presented by Liang et al. [50]. The detection of α-fetoprotein based on a sandwich immunoassay by immobilizing a primary α-fetoprotein antibody on the SPR sensor surface of a polymeric film employing magnetite-gold-α-fetoprotein antibody conjugates as the amplification reagent was developed by them. Calibration curve of magnetite-gold-α-fetoprotein secondary antibody conjugates amplification for α-fetoprotein detection to produce a correlation in the range of 1.0–200.0 ng/mL with a LOD value 0.65 ng/mL was obtained. Through the use of magnetite-gold-α-fetoprotein antibody conjugates as an amplifier, important increment in sensitivity was provided.

Cardiac biomarkers detection acts a significant function in the diagnosis and risk stratification of patients with chest pain and acute myocardial infarction. Myoglobin, creatine kinase-myocardial band, and cardiac troponins are the markers used to diagnose acute myocardial infarction. SPR sensor combined with the advantages of molecular imprinting-based synthetic receptors was developed by Osman et al. [51]. Myoglobin imprinted polymeric film produced onto the SPR sensor interacted with protein solutions in the concentration range from 0.1 μg/mL to 10 μg/mL (Fig. 10.4a). They observed a fast response when the myoglobin sample solution

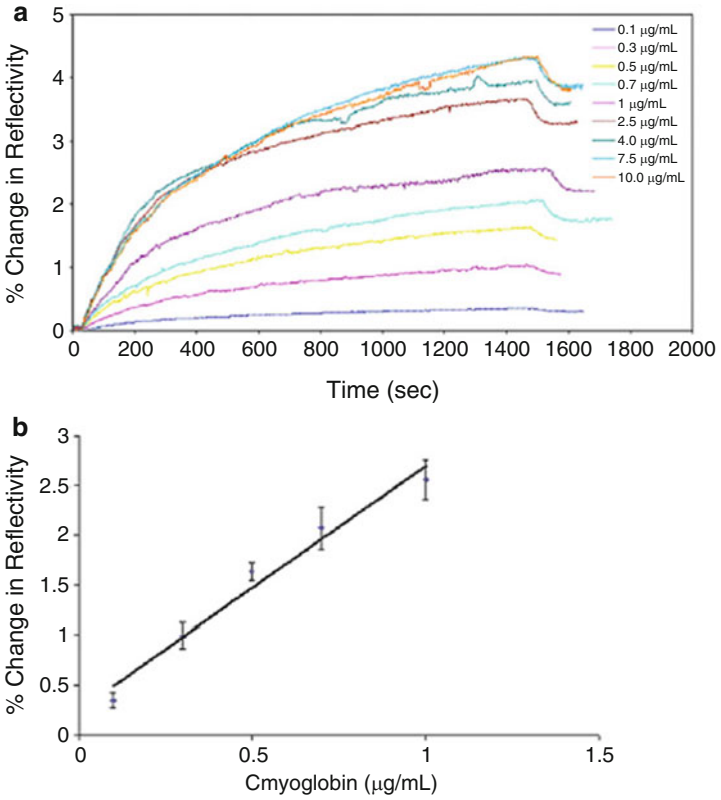

Fig. 10.4 (**a**) The sensorgrams and (**b**) concentration dependency of the SPR sensor [51]

arrived at the SPR sensor. They also observed that the SPR sensor response was increased when the concentration of myoglobin was increased as well. Figure 10.4b described the linearity of the SPR sensor in the range of 0.1 μg/mL–1.0 μg/mL. They calculated the LOD and limit of quantification (LOQ) values as 26.3 ng/mL and 87.6 ng/mL, respectively. They also used the SPR sensor to detect myoglobin in serum. They diluted the blank solution with a 1/15 ratio and spiked the samples with 0.3, 0.5, 0.7, and 1.0 μg/mL myoglobin in the same dilution ratio. They determined the myoglobin concentration in the diluted serum as 42.6 ng/mL. Their results showed that the SPR sensor could determine the myoglobin concentration with high accuracy when compared with the ELISA method (58.3 ng/mL).

Lysozyme detection has gained importance because the alteration of lysozyme levels can be used as a marker for some diseases such as meningitis, leukemia, several kidney problems, and rheumatoid arthritis. Lysozyme imprinted polymeric nanoparticles, which were modified on the SPR sensor, were represented by Sener et al. [52]. They detected lysozyme in both aqueous and natural complex sources even if lysozyme concentration was as low as 32.2 nM. They calculated the LOD, K_a, and K_d values as 84 pM, 108.71 nM^{-1}, and 9.20 pM, respectively.

Pregnancy-connected plasma protein A2 is a metalloproteinase that acts multiple roles in fetal development and postnatal growth. Bocková and coworkers presented the SPR sensor for plasma protein A2 detection in blood samples by using both single surfaces referencing method and sandwich assay with functionalized gold nanoparticles [53]. They also demonstrated that this SPR sensor had an ability to detect plasma protein A2 in blood plasma with 3.6 ng/mL LOD value. The researchers characterized the performance of the SPR sensor and evaluate its cross-reactivity to a plasma protein A2 analogue.

Alzheimer's disease is defined by the amyloid β-protein oligomerization as an early event. There is a risk of overdiagnosis employing sequence-specific antibodies oppose to toxic fibrillary and monomeric amyloid β-protein by current diagnostic methods. Murakami et al. gave much attention to developing more accurate diagnostics such as conformation-specific antibodies against neurotoxic amyloid β-protein oligomers [54]. They observed that the ratio of toxic to total amyloid β-protein in the cerebrospinal fluid of Alzheimer's disease patients was higher than in control molecules as determined by ELISA.

Selective laminin-5 determination using SPR sensor that depended on the specific interaction of laminin-5 with rabbit polyclonal antibody was performed as a new method by Sankiewicz et al. [55]. They showed that the reply range of the SPR sensor was between 0.014 and 0.1 ng/mL and calculated LOD value as 4 pg/mL. They also determined the laminin-5 concentration in blood plasma to examine the potential application of the SPR sensor. They compared the results with ELISA method, and according to their results, the plasma samples of bladder cancer patients gave more concentrated results with SPR sensor than by ELISA. The study showed that there is a clear difference in laminin-5 concentration in healthy people and patients with bladder cancer.

A self-assembled monolayer of protein chimeras to display an array of oriented antibodies on a microelectronic sensor for influenza nucleoprotein detection was described by Brun and coworkers as a new strategy [56]. They characterized their system with the structural and functional features of the bio-interface by SPR. Furthermore, they also showed that the non-covalent structure could render the dissociation of binding antibodies irreversible by chemical cross-linking in situ without attacking the antibody function.

Liu and colleagues demonstrated a fiber-optic SPR sensor that depended on the smartphone platforms by connecting the optical and sensing elements to a phone case [57]. They showed that the SPR sensor could be installed or removed from the smartphones. They also exhibited the accuracy and repeatability measurements by detecting several concentrations of antibody binding to a functionalized sensing element for smartphone-based SPR platform performance. Validation experiments resulted through contrast experiments with a commercial SPR instrument.

Rapid and reliable detection of procalcitonin by a molecularly imprinted polymer on the gold surface of SPR sensor was reported by Sener et al. [58]. According to this method, procalcitonin molecules were attached with the polymeric solution containing 2-hydroxyethylmethacrylate and ethylene glycol dimethacrylate on the SPR sensor after immobilization onto the glass slide, and then the polymerization

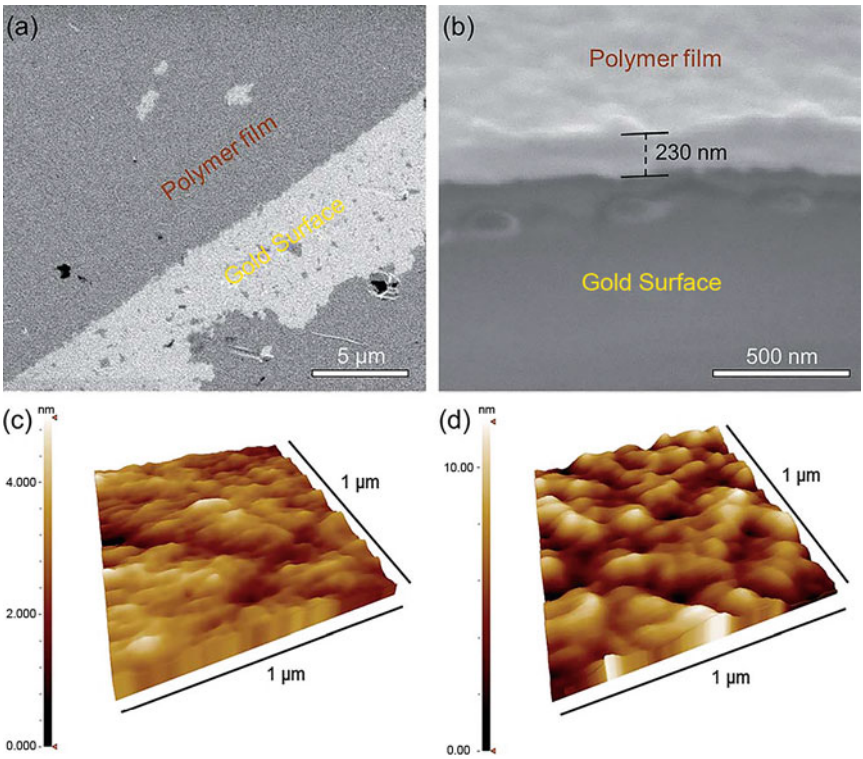

Fig. 10.5 (**a** and **b**) SEM images of procalcitonin imprinted polymer nanofilm, AFM images of (**c**) bare, and (**d**) procalcitonin imprinted SPR sensor surfaces [58]

process was initiated via UV light. Specific molecular binding sites were obtained after the removal of procalcitonin. They first characterized the SPR sensor (Fig. 10.5) and used for detection studies. The detection studies by using procalcitonin solutions in phosphate buffer and artificial blood plasma at diverse concentrations were performed after the characterization of the micro-contact imprinted SPR sensor. They also showed that the SPR sensor could detect low concentration of procalcitonin in both phosphate buffer and artificial blood plasma with a LOD value of 9.9 ng/mL.

5.2 Hormone Detection

Diagnosis of the endocrine diseases is generally difficult and needs to directly monitor and make measure hormone levels. Hormone detection demonstrates the talent of SPR technology to supply attractive answers in this clinical field and is provided in some recent studies by different groups [59].

Cenci et al. produced a library of molecularly imprinted nanoparticles to target the N-terminus of the hormone hepcidin-25 whose serum levels correlate with iron

dis-metabolisms and doping. They immobilized the molecularly imprinted nanoparticles onto the NeutrAvidin™ SPR sensor chip [60]. They studied the responses of the SPR sensor to hepcidin-25 and observed the low K_d values for the interaction of molecularly imprinted nanoparticles with hepcidin-25, but none for the molecularly imprinted nanoparticles and non-regulative hepcidin-20. They acquired the linearity with the logarithm of hepcidin-25 concentration in the range of 7.2–720 pM, and LOD value was 5 pM.

Zhang and coworkers developed a water-compatible molecularly imprinted polymer film with suitable monomers, cross-linker, polystyrene nanoparticles, and template for testosterone detection in urine [61]. Artificial urine and human urine incubation on the molecularly imprinted polymer film and the non-imprinted film was used to estimate undetectable non-specific adsorption. Testosterone detection was recorded with the LOD value down to 10^{-15} g/mL, which was regarded as one of the lowest values among the SPR sensors. The selectivity studies of molecularly imprinted polymer film were performed with the similar molecules to the testosterone such as progesterone and estradiol. They also showed that the SPR sensor had extreme stability and reproducibility over 8 months of storage at 25 °C which was better than protein-based sensors.

Vashist and his collaborators prepared SPR sensor for rapid immunoassay of procalcitonin with high detection sensitivity and reproducibility [62]. The activated protein A was dispensed on a potassium hydroxide-treated gold-coated SPR sensor surface and bound covalently in 30 min. They calculated the values of LOD and LOQ of the SPR sensor as 4.2 ng/mL and 9.2 ng/mL, respectively. They also claimed that the SPR sensor was capable of detecting procalcitonin in real sample matrices and patient samples with high precision.

Trevino et al. prepared the one and multiple analyte SPR systems for two gonadotropic hormones and luteinizing hormone from untreated human urine [63]. They found the lowest LOD values as 8 mIU/mL and 14 mIU/mL for luteinizing hormone and gonadotropic hormones in human urine. They also searched that the stability of the SPR sensor signals through more than hundred trials. They tested the comparison of the calibration curves for the three different SPR sensors. They observed that the reproducibility of chip-to-chip was exceptional and calculated the mean variation coefficients of 4.2% and 3.7% for gonadotropic hormones and luteinizing hormone, respectively.

The same research group has carried out studies to determine four pituitary hormones such as human thyroid-stimulating, growth, follicle-stimulating, and luteinizing hormones by using a portable SPR sensor [64]. They displayed the performance of the SPR sensor in different solutions ranging from 1 to 6 ng/mL. They injected the growth hormone samples to produce SPR signal due to the phosphate buffer and non-specific binding of serum components. They also obtained a calibration curve and the analytical characteristics. Their SPR sensor allowed the growth hormone determination in serum with different concentrations. Their results showed that the SPR sensor was suitable for practical and fast clinical diagnosis of growth hormone deficiency.

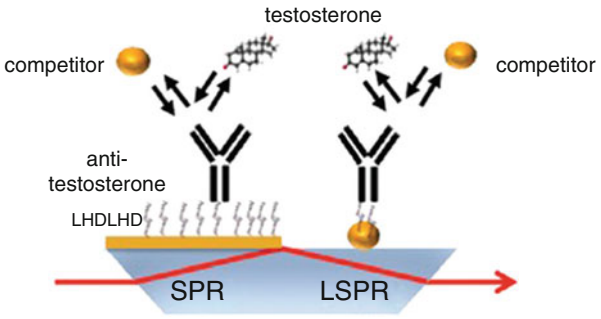

Fig. 10.6 Scheme of SPR and localized SPR systems on testosterone detection [66]

A fiber-optic SPR sensor was presented by Srivastava et al. for endocrine disruption biomarker detection [65]. They employed antibody immobilization on the SPR sensor surface. They prepared various concentrations of the biomarker in the range of 1.0–25 ng/mL and also performed control experiments with similar molecules. They found the LOD and sensitivity values of the SPR sensor as 1 ng/mL and 0.48 ng/mL in aqueous solution, respectively. Their fiber optic of the SPR sensor was fixed in a flow cell, and the flow cell had the supplies for sample input and output. Acetone-soaked optical tissue was used to wipe the ends, after fixing the fiber into the flow cell. Tungsten-halogen light source producing polychromatic light was coupled to the input end of the SPR fiber sensor probe with the help of a microscope objective of 0.65 NA to save the SPR sensorgram.

Yockell-Lelièvre and coworkers reported two sensing platforms utilizing functionalized gold nanoparticles to detect testosterone with SPR and localized SPR [66]. They provided a study based on the surface chemistries that can produce stable detection systems before detecting testosterone by employing four-channel SPR sensor system. As shown in Fig. 10.6, the SPR sensor was produced on a film on the prism, while the localized SPR sensor was originated by a monolayer gold nanoparticles immobilization on the prism. Development of the SPR and localized SPR sensors was depended on the competition of free testosterone with a testosterone-biotin. The basis of the competition assay for both SPR and localized SPR sensors relies on gold nanoparticles immobilized with testosterone-biotin. When high testosterone concentrations were applied to the SPR and localized SPR systems, the binding of a competitor to the SPR and localized SPR sensor was declined, and thus they observed a lower response.

Trade-offs between sensitivity, specificity, experiment range and time, instrumentation, sample carrier, and storage requirements with challenges for several SPR sensor applications were discussed by Sanghera et al. [67]. They calculated the LOD value of SPR sensor as 0.5 nM. They tested the insulin binding features of SPR sensor that called Protean Bio-Rad XPR36 at different pH values. They applied the insulin sample to the SPR sensor with a contact time of 300 s and a dissociation time of 400 s, at a flow rate of 25 μL/min at pH 7. They extended contact and dissociation time to improve sensitivity with same flow rate. They evaluated insulin concentration effect

on the produced signal intensity by SPR, and they declared that the more extensive contact and association times permitted, the better distinction for the different concentrations than the shorter times.

5.3 Nucleic Acid Detection

Many nucleotidic molecules of interest in medical diagnostics have been determined by nucleic acid that depended on SPR sensors. Eukaryotic chromosome ends are defended from undesired degradation, recombination, or end-to-end fusion by telomerase cap. Sharon and coworkers described the telomerase activity in human cells for the analysis of sensor involves the telomerase activity [68]. Telomerase activity was detected by their amplified SPR sensor. They did the telomerization in the mixture of the telomerase and the nucleotide, which results in the formation of telomeres on the SPR sensor surface modified with gold film-coated glass slides, and altered the surface dielectric properties that resulted in a shift in the SPR spectrum. As represented in Fig. 10.7a–d, they detected the telomerase extracted from 18 293 T cells/μL by using SPR spectra and observed the reflectance changes by sensorgrams corresponding to the different numbers of 293 T cell extracts.

Diltemiz et al. prepared SPR sensor for recognition of DNA. They reported that not only the detection of guanosine and guanine but also the DNA sequencing assay is possible with molecularly imprinted SPR sensor [69]. The binding experiments by ligand and guanosine and guanine imprinted polymers with respect to guanine and double-strand DNA were also included in their studies. They calculated the affinity constants for guanosine and guanine imprinted SPR sensors by plotting adsorption isotherms of adenosine, guanosine, guanine, adenine, single-strand DNA, and double-strand DNA, and the results were shown in Fig. 10.8.

The computationally assisted method was suggested based on the aptamer and protein interaction with the purpose of well-organized screening and selection of aptamers by Turner and collaborators [70]. They generated the computationally derived binding scores by screening a formed library of mutated DNA sequences based on the beginning from the data on the 15-mer thrombin-binding aptamer. They chose thrombin-binding aptamer and three other mutated oligonucleotides according to their binding score. They compared the analytical behaviors of the four oligonucleotide sequences employing signal amplitude, sensitivity, linearity, and reproducibility by reducing the ionic strength in order to match the simulated condition. They showed that their experimental results were in agreement with the simulation findings.

Highly infectious and rapidly spreadable through contact, bacterial meningitis is a dangerous infection of the meninges of the brain and spinal cord, which can even cause death. The report about SPR sensor was presented by Kaur and coworkers to detect *Neisseria meningitidis* DNA by utilizing laboratory assembled SPR sensor [71]. In their study, they immobilized the single-stranded probe DNA on SPR sensor surface. They provided the change in optical features at gold-zinc oxide interface by the DNA hybridization on the SPR sensor surface. A continuous shift in the dip angle of the SPR reflectance because of the dielectric properties changes of zinc

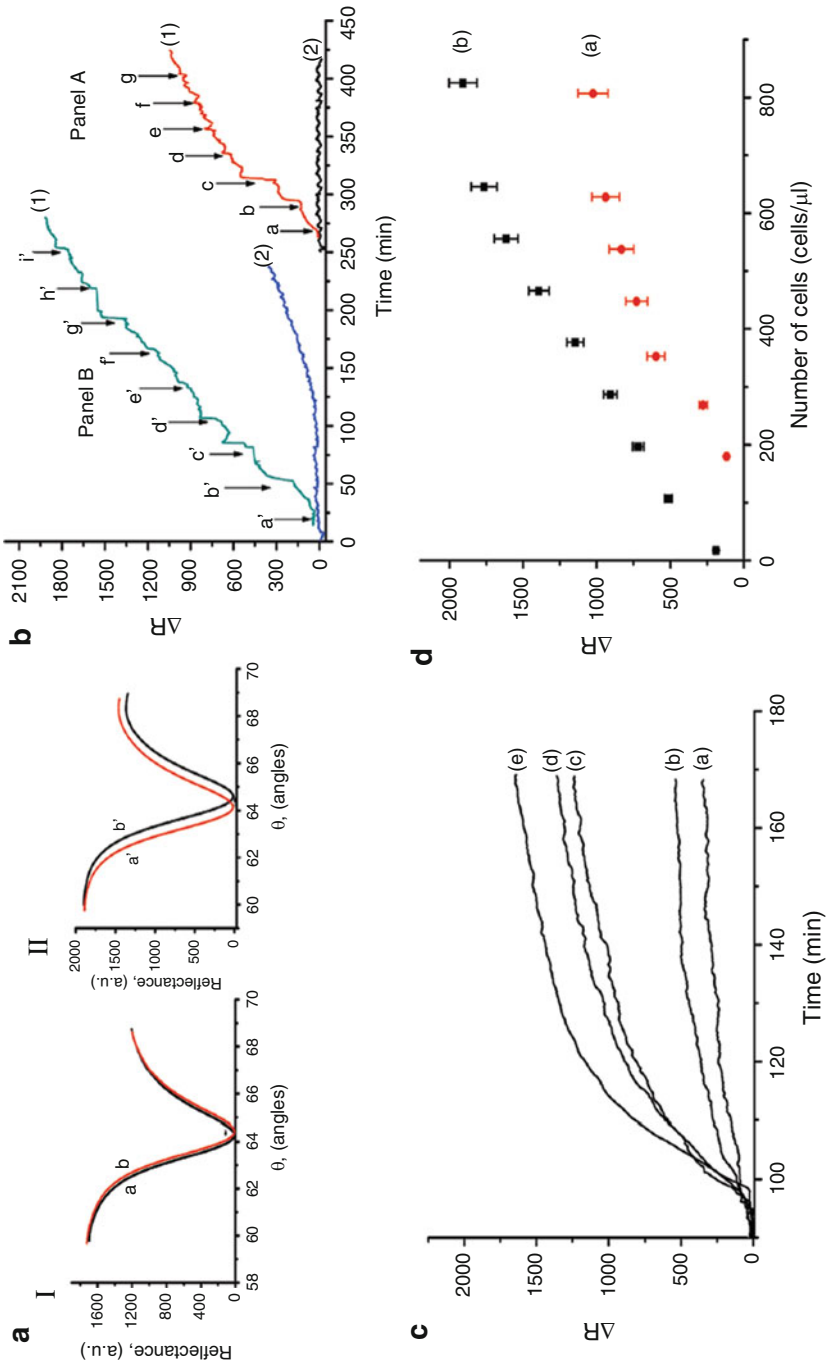

Fig. 10.7 The reflectivity responses in different steps [68]

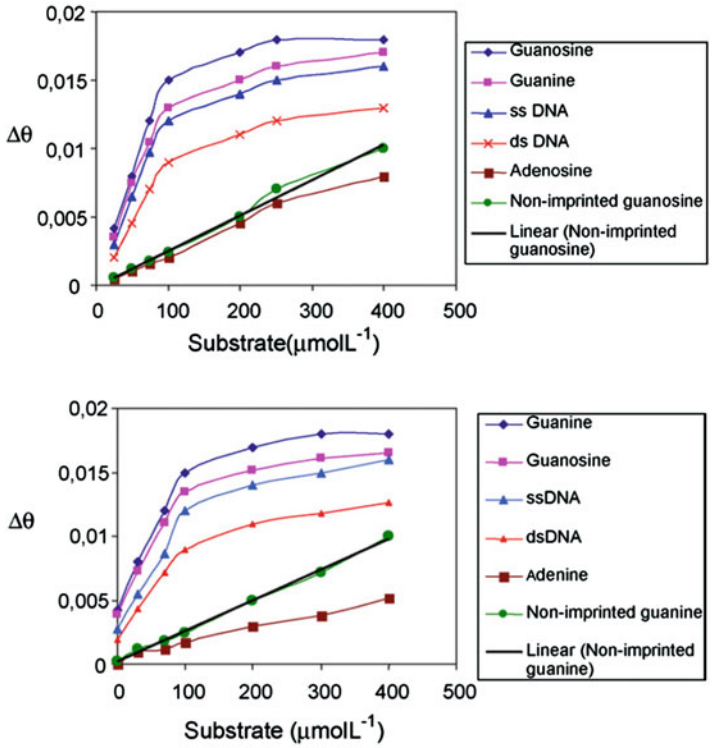

Fig. 10.8 The adsorption isotherms and selectivity of molecularly imprinted SPR sensors [69]

oxide matrix owing to the interaction between complementary DNA strands was observed with increase in the concentration of DNA. Furthermore, a continuous decline in the value of R_{min} with an increase in oligonucleotide concentration was also observed, which showed the binding between the probe and DNA. They obtained a linear response toward meningitides DNA over the concentration range from 10 to 180 ng/μL with a LOD value (5 ng/μL).

DNA arrays are priceless devices for sensing applications such as diagnostic DNA detection and gene expression analysis. Untagged oligonucleotide targets adsorbed to the array molecules can be detected by SPR imaging system. A template-directed polymerase extension of a surface array element was described as a new method by Gifford and coworkers [72]. They claimed that it is possible to obtain 10–100 attomole of polymerase outcome, representing as low as 0.25% of a monolayer by using their technique. Their system allowed detecting DNA present in low amounts in a sample with the partially unknown sequence. As seen in Fig. 10.9, they spotted the different ratios of probe DNA and T^{30} onto the glass surface above the gold spots and showed the binding of nanoparticles to the surface-bound DNA by a percent reflectivity change with the line profile indicated by the black line at the left inset.

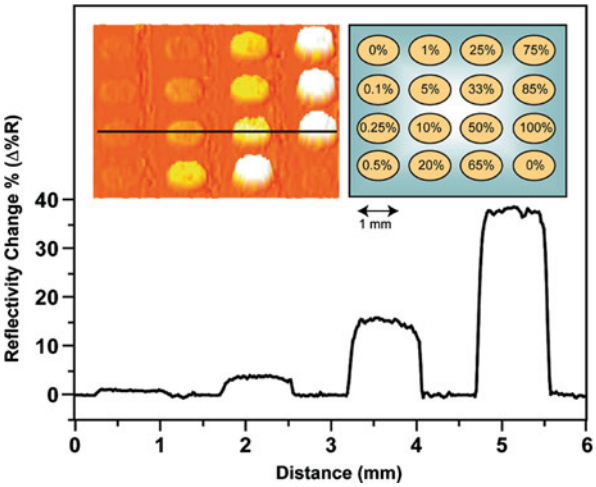

Fig. 10.9 The nanoparticle-based SPR imaging [72]

D'Agata et al. represented a detection strategy for genomic DNA that associated with the β-thalassemia disease [73]. Direct fluxing of DNA samples into each of the SPR imaging fluidic systems to let the direct interaction of each of the samples with different probes complementary to the normal and mutated DNA sequences was performed (Fig. 10.10). They declared that these different probes were functional both to distinguish between normal, homozygous, and heterozygous DNAs as well as to keep away the use of external controls which were difficult to be acquired for this application. Normal, homozygous, or heterozygous DNAs were each permitted to interact with the two different PNA probes, and obtained specific SPR imaging response patterns provided a robust experiment control.

The aptasensor that depended on the inactivation of surface plasmon enhancement of fluorescent probes modified to gold nanoparticle-bound aptamers was reported by Cho and colleagues [74]. They claimed that this sensing system measured the target directly at the clinically relevant range from 1.25 pM to 1.25 mM with high specificity and stability. Their results showed a good agreement within the limit of the ELISA kit for clinical sample experiments. The unfolded VEGF165 aptamer was bound to poly-L-lysine-coated gold nanoparticle surface as electrostatically in the lack of target molecules as shown in Fig. 10.11a. In addition Fig. 10.11b reflected that the interactions of the VEGF165 aptamer to its target induced the reversible conformation to modify the aptamer and the declined electrostatic binding force. An irreversible detachment of the aptamer from the GNP surface was caused by the target-binding interaction of the aptamer, which avoided the SEF effect of Cy3B (Fig. 10.11c).

5.4 Whole Cell Detection

Dengue is a crucial febrile disease, which is induced by the dengue virus and inserted into a host by a female *Aedes aegypti* mosquito and globally identified as one of the

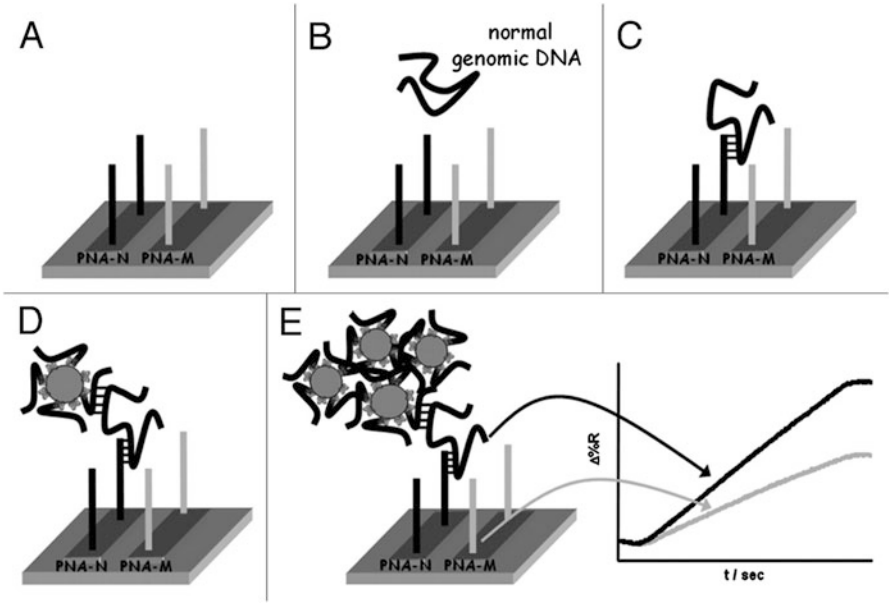

Fig. 10.10 The description of the nanoparticle-enhanced SPR imaging strategy [73]

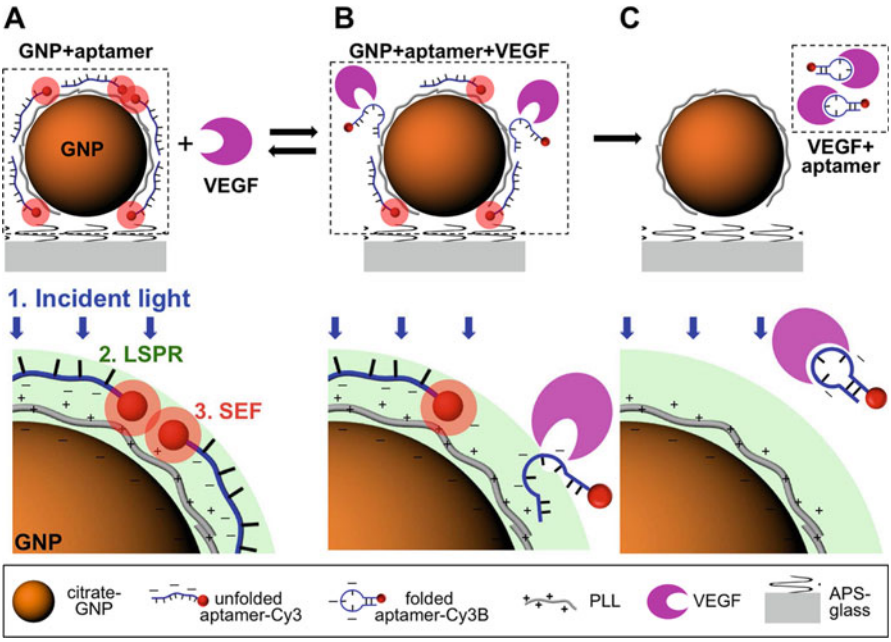

Fig. 10.11 The detection mechanism scheme of the aptasensor for VEGF165 [74]

most important vector-borne diseases. Anti-dengue virus detection in serum samples was proposed as a rapid method based on SPR by Jahanshahi and colleagues [75]. They claimed that their system, known as 10 min detection of immunoglobulin M-based dengue diagnostic test, could be applied rapidly and easily. They used different dengue virus serotypes as ligands on SPR sensor. They obtained 83–93% sensitivity, and 100% specificity for 1 ml from a patient was needed to indicate SPR angle variation to determine the ratio of each dengue serotype in samples.

Adenovirus detection was carried on by utilizing plastic and natural antibodies to refer three different strategies investigations. The implementation of a molecularly imprinted method for detection of viruses with the combination of sensors was described by Altintas et al. [76]. They used the SPR sensor as affinity receptor with the concentration range of 0.01–20 pM for the adenovirus detection and found the LOD value as 0.02 pM. They also performed the conduction of cross-reactivity studies with MS2 phage as a control virus and achieved high specificity.

Clinical diagnosis of canine distemper virus causing viral disease that influences dogs and many other carnivores is hard because of the broad spectrum of signs that may be confounded with other respiratory and enteric diseases of dogs. Basso et al. developed an SPR sensor to detect canine distemper virus [77]. They obtained a sensorgram after modification steps and the canine distemper virus concentration with a linear range from 1.1 to 116.0 ng/mL. They claimed that their SPR sensor showed a good reproducibility.

Avian influenza virus detection is needed because it causes H5N1 influenza infection in animals and humans. Bai and coworkers made research based on an SPR sensor for avian influenza virus H5N1 detection [78]. They fabricated the SPR sensor by using aptamers and then modified the gold surface of the SPR sensor coated with streptavidin. According to their results, the aptamers captured avian influenza virus H5N1 in a sample solution, which caused a refraction index increase, and the refraction index value was linearly related to the avian influenza virus concentration in the scale of 0.128 to 1.28 haemagglutination unit.

SPR sensor was developed to detect hemagglutinin which is a major protein of influenza A virus by Diltemiz et al. [79]. They modified SPR sensor surfaces with thiol groups and then 4-aminophenyl boronic acid, and the sialic acid mixture was immobilized on sensor surfaces. They employed aqueous hemagglutinin solutions to determine binding features of sensors to influenza A virus. They also calculated LOD values for SPR sensor as 1.28×10^{-1} μM, in the 95% confidence interval.

Molecularly imprinted SPR sensor to target the bacteriophage MS2 was developed by Altintas et al. [80] to detect waterborne viruses. They obtained an excellent affinity between the artificial ligand and the target (Fig. 10.12a). As shown in Fig. 10.12b, molecularly imprinted SPR sensor surface was renewed by using 0.1 M HCl (R1) and 20 mM NaOH (R2). In addition, blue line reflected the phage binding on molecularly imprinted SPR sensor, whereas red line represented the MS2 phage binding on molecularly imprinted SPR sensor in Fig. 10.12c. According to their results, they claimed that a regenerative molecularly imprinted virus detection SPR sensor was successfully promoted and provided an alternative and specific detection technology for the waterborne viruses leading to high disease and death rates all over the world.

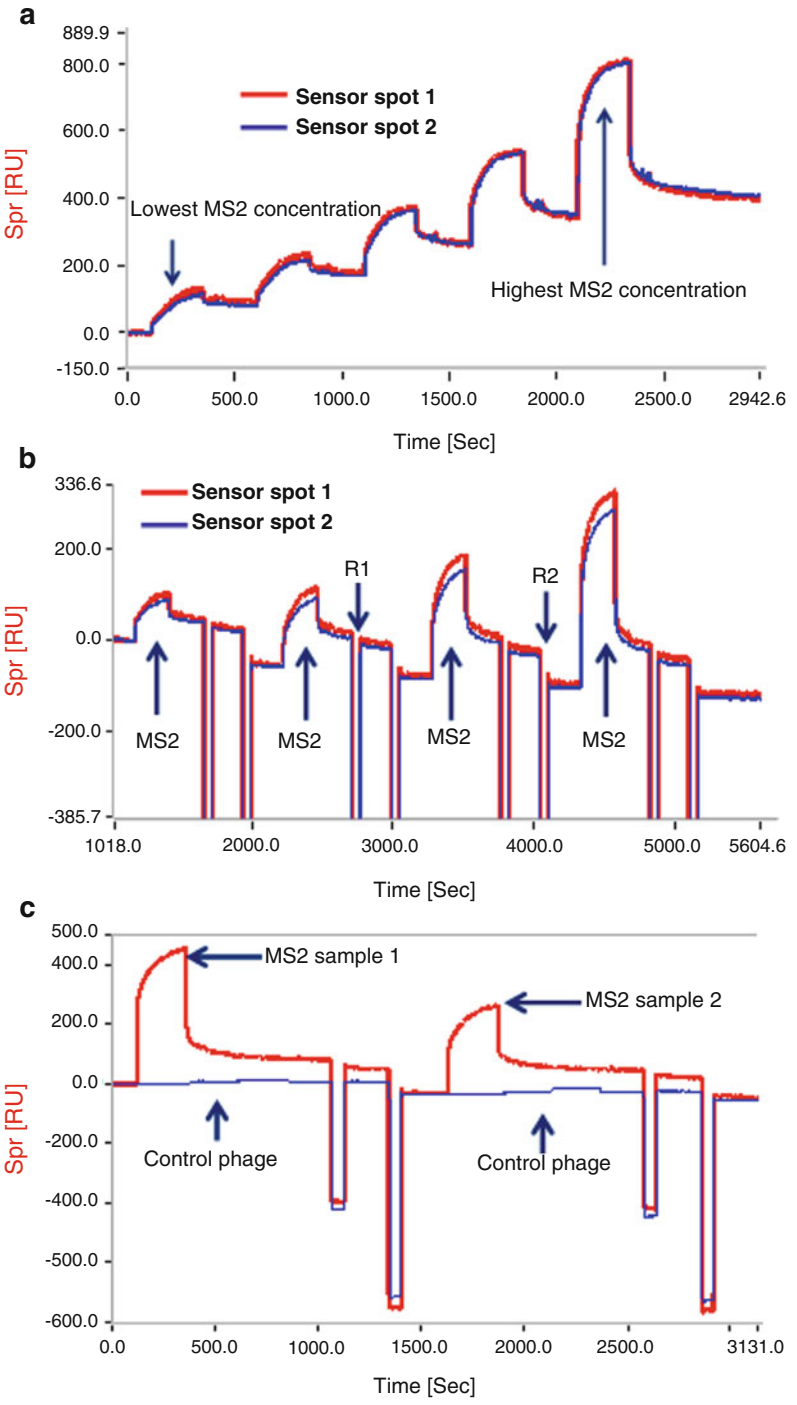

Fig. 10.12 The sensorgrams of the (**a**) continuous, (**b**) regenerative virus binding experiments, (**c**) cross-reactivity test using phage as control [80]

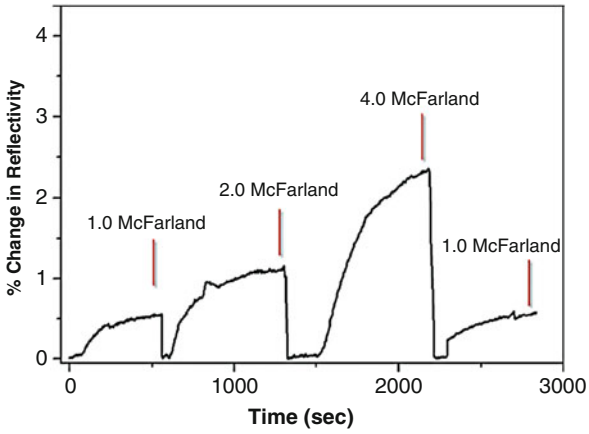

Fig. 10.13 The sensorgrams of the SPR sensor against the apple juice spiked with *Escherichia coli* at different concentrations [82]

Riedel and his research group offered SPR sensor to develop a new-generation medical diagnostic technologies [81]. They introduced an SPR sensor based on diagnosing different stages of Epstein–Barr virus infections in clinical serum samples and showed that the detection of the antibodies against three different antigens present in the virus was achieved by their study. The interference of the fouling from serum during the measurements was prevented by coating the SPR sensor with an antifouling layer of a polymer brush. Attachment of receptors by hybridization of complementary oligonucleotides allowed the SPR sensor surface regeneration after measurements by disrupting the complementary pairs above the melting temperature of oligonucleotides.

The detection of pathogenic bacteria is necessary to prevent infections and also life-threatening illnesses. Yılmaz et al. described a molecularly imprinted SPR sensor to detect *Escherichia coli* from water sources [82]. They choose amino acid-based molecule to provide similar interaction as in natural antibodies. After the polymerization, they first characterized the SPR sensor surface and then obtained a linear behavior as 98.79% at different *Escherichia coli* concentrations in the range of 0.5–4.0 McFarland. They also performed the real sample experiments with apple juice (Fig. 10.13). According to their results, the increment of the concentration of *Escherichia coli* gave rise to an increment in SPR sensor reflectivity.

Wang and collaborators displayed an SPR sensor for *Escherichia coli* O157: H7 detection [83]. In their system, *Escherichia coli* O157: H7 cells and goat polyclonal antibodies for *Escherichia coli* O157: H7 were incubated, and then the *Escherichia coli* O157: H7 cells were removed by a centrifugation step. Their results exhibited that the signals were oppositely correlated with the concentration of *Escherichia coli* O157: H7 cells in a scale from 3.0×10^4 to 3.0×10^8 CFU/mL. They compared the SPR sensor and ELISA to capture *Escherichia coli* O157: H7, and the LOD value was decreased by one order of magnitude. They commented that their method simplified bacterial cell detection and has the capacity to provide an efficient option for detecting *Escherichia coli* O157: H7 and other pathogens.

Karoonuthaisiri et al. aimed to display how filamentous M13 bacteriophages expressing 12-mer peptides could work in SPR sensor to detect the foodborne bacterium *Salmonella* [84]. They examined different factors for the successful

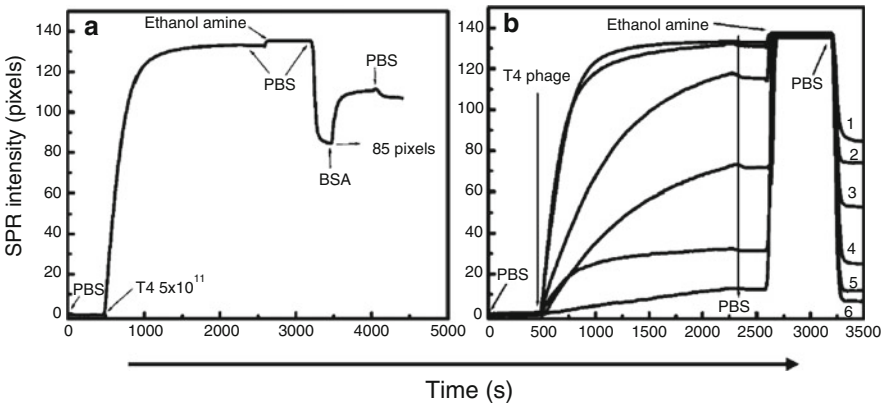

Fig. 10.14 The sensorgrams of the SPR sensor for (**a**) covalent immobilization of T4 phage, (**b**) covalent immobilization of different concentrations of T4 phages [85]

bacteriophage detection by SPR sensor. They used citric–Na_2HPO_4 buffer at pH 3.0–7.4 as an immobilization buffer for four different bacteriophage clones (MSal020401, MSal020404, MSal020417, and LM0205P01H01). They obtained low cross-reactivity and LOD values of 8.0×10^7 and 1.3×10^7 CFU/mL for one-time and five-time. Feasibility of label-free SPR assay for rapid pathogen detection by employing M13 bacteriophages expressing target-specific peptides was proved by their studies.

A T4 bacteriophage assay and SPR system were developed by Arya et al. as a specific receptor and transduction system to detect *Escherichia coli* K12 bacteria [85]. They used dithiobis(succinimidyl propionate) to immobilized T4 phages onto gold SPR sensor surfaces by utilizing self-assembled monolayer. They demonstrated that SPR sensor could detect the *Escherichia coli* K12 with high specificity against non-host *Escherichia coli* NP10 and NP30. They obtained the maximum host bacterial capture when T4 phages concentration was used as 1.5×10^{11} PFU/mL for immobilization. Figure 10.14a showed the plot of the SPR sensor response versus time induced by the chemical modification of the phages on the SPR sensor surfaces. Also, they recorded the responses of the SPR sensor for the binding properties by employing different concentrations of T4 phage solution. The number of curves from 1 to 6 had 5×10^{11}, 1.5×10^{11}, 1×10^{11}, 8×10^{10}, 5×10^{10}, and 1×10^{10} PFU/mL concentration in Fig. 10.14b.

Kuo et al. developed SPR sensing system for differentiation of cell detection in living cells due to the differences of the cell surfaces optical features [86]. Evaluation of the mesenchymal stem cells osteogenic differentiation by SPR system application was reported, and a linear relationship with a high correlation coefficient between the duration of osteogenic induction and the difference in refractive angle shift was observed. They used a He-Ne laser that penetrated through a polarizer and a beam splitter. The one was detected by a photodiode, while the other one was coupled by a prism for generation of surface plasmon wave by which the angle shift was detected

with a photodiode. At the end of the study, they emphasized that their SPR system could define osteogenic maturation of mesenchymal stem cells in a live cell as a label-free manner without cell breakage.

Yanase and collaborators reported that huge changes of refractive index by living cells could be detected with SPR sensor systems [87]. They performed the refractive index visualization of individual living cells by the prepared SPR imaging sensor. Developed SPR imaging sensor could detect reactions of individual rat basophilic leukemia cells and mouse keratinocyte cells in response. Furthermore the reactions of individual human basophils isolated from patients in response to an allergen could be detected also by the SPR sensor system. They obtained that SPR signals by the binding of anti-DNP IgE and DNP-HSA to rat basophilic leukemia cells were cultured on the surface of the SPR sensor. According to their results, the SPR system could visualize several stimuli, inhibitors effect, and conditions on cell reactions as a change of intracellular refractive index distribution at single cell levels.

The same research group also presented an SPR imaging system that had a multiple sensing with a hydrophobic membrane to detect basophils that were isolated from patients [88]. They only used a microliter of patient's blood and detected specific reactions of human receptor-expressing mast cells in response to antigens. SPR imaging system might be an excellent throughput screening system of type I allergy, not only for freshly prepared basophils but also for sera stored in clinical practices, and was claimed as a functional device for their studies. The refractive index changes of receptor-expressing mast cells were observed by the SPR imaging sensor. In addition, they obtained the time course of refractive index changes in the area with receptor-expressing mast cells in the presence or absence of anti-IgE.

5.5 Drug Detection

High affinity synthetic receptors can be used to detect drugs in clinical diagnosis studies. Altintas et al. prepared SPR sensors by using molecularly imprinted polymers that were combined with computational simulation [89]. They first synthesized the metoprolol imprinted polymers and then produced SPR sensor to sensing metoprolol. Metoprolol is a blocker drug that is detected by SPR sensor in the range of 1.9 ng/mL–1.0 μg/mL with a correlation coefficient of 0.97. They also developed a regeneration method for the reusability of SPR sensor. They calculated the K_d as 1.35×10^{-10} M by using Langmuir isotherm model. They also determined the stability experiment by measuring the size and quality of the receptor periodically during 6 months. Their results showed the success of computationally modeled receptor with SPR sensor for drug detection and monitoring.

The same research group members synthesized nanoparticles by using SPR sensor that are based on molecular imprinting method for diclofenac detection [90]. They measured the size of nanoparticles as around 132.3 nm with 0.1 of polydispersity index that confirms the property of the nanoparticles. After that, they immobilized the nanoparticle onto the SPR sensor surface via covalent coupling with EDC/NHS and detected diclofenac in the range of 1.24–80 ng/mL by the SPR

sensor. They also performed the efficiency of SPR sensor by using functionalized diclofenac with gold nanoparticles and free diclofenac. Glycine–hydrochloric acid solution was used to regenerate the SPR sensor surfaces. Subsequent analyses performed by them indicated the stability of the sensor surface. They obtained the K_d value as 1.48×10^{-9} M. At the end, they examined the cross-reactivity studies against other pharmaceuticals by employing the SPR sensor.

Yockell-Lelièvre and his collaborators achieved to detect methotrexate with a plasmon-coupling assay [91]. They immobilized the gold nanoparticles onto the sensor inserted in a portable four-channel localized SPR reader and competition of free methotrexate and folic acid. They claimed that their sensor system allowed measuring methotrexate according to the total internal reflection plasmonic spectroscopy. Color changes can be visible to the naked eye for methotrexate by the huge shifts of the plasmon-coupling assay.

Pernites et al. developed the chemosensitive sensor to detect naproxen, paracetamol, and theophylline by employing non-covalent molecularly imprinted polymers [92]. Monofunctional and bifunctional hydrogen bonding terthiophene and carbazole monomers series were compared for imprinting these drugs. They characterized the prepared surfaces by several techniques and confirmed the templating and release of the drug from the cross-linked conducting polymer film.

Pernites and coworkers also prepared a sensor to detect theophylline by molecularly imprinted polymeric film [93]. They monitored the formation of the electropolymerized molecularly imprinted polymeric film by electrochemical SPR sensor allowing examination of the simultaneous changes in electrochemical and optical properties of the film (Fig. 10.15). They obtained a calibration curve of the SPR sensor for theophylline detection with a 10–50 μM^{-1} range and LOD value of 3.36 μM^{-1}.

Golub and collaborators used SPR sensor based on metallic nanoparticles for cocaine detection by using aptasensor configuration [94]. As seen in Fig. 10.16, their sensors were depended on utilizing two anti-cocaine aptamer subunits, where one subunit was assembled on a gold support, acting as an SPR-active surface, and the second aptamer subunit was labeled with other nanoparticles (Pt, CdS, Au). In different configurations, quantitative analysis of cocaine was estimated by the addition of cocaine resulting in the formation of supramolecular complexes between the nanoparticle-labeled aptamer subunits and cocaine on the metallic surface. Detection of cocaine by the electrocatalyzed reduction was exhibited by the complex formation between the supramolecular Pt nanoparticles aptamer subunits and cocaine molecules. In addition, the generated photocurrents by the CdS nanoparticle-labeled aptamer subunits-cocaine complex also allowed the photoelectrochemical detection of cocaine. They showed that all aptasensors were able to analyze cocaine with a LOD value in the range of 10^{-6}–10^{-5} M.

Wang et al. investigated an application of case study that depended on Mach–Zehnder configuration and SPR sensor for drug screening, calculating reaction kinetic constants, inhibition effect and cytotoxicity analysis [95]. They selected cetuximab as a target molecule and measured with a sensitivity of 10^{-6} and stability of 6×10^{-7} refractive index unit in 80 min in SPR sensor. Reaction kinetic constants of cetuximab binding to epidermal growth factor receptor was calculated as $1.75 \pm 0.29 \times 10^{-3}$ S^{-1}

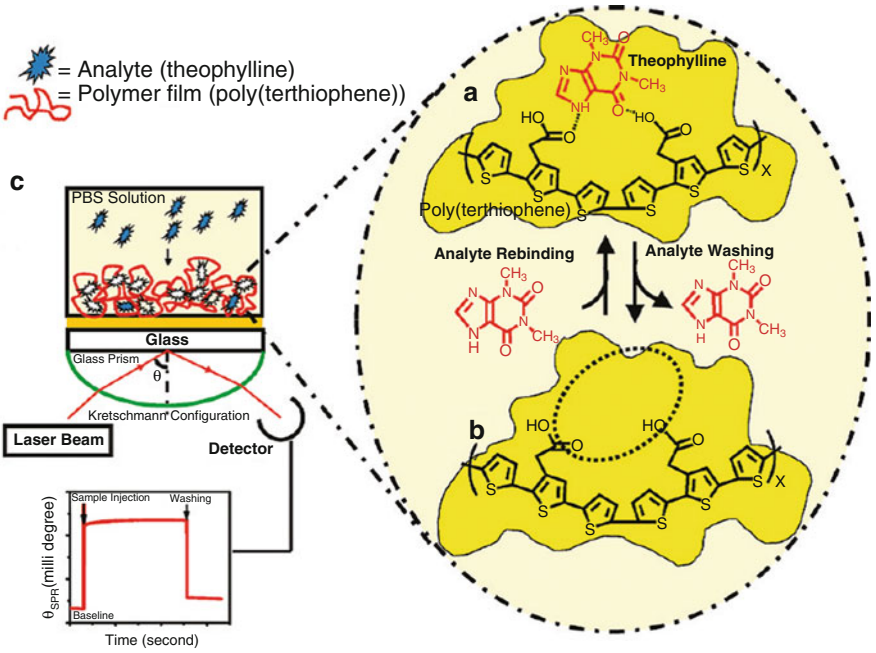

Fig. 10.15 (**a**) Molecular imprinting of theophylline, (**b**) formation of the cavity after washing, (**c**) SPR setup for sensing of theophylline [93]

and 4.19 ± 0.58 nM. Their results showed that cetuximab could block epidermal growth factor receptor binding to its two ligands, epidermal growth factor, and epidermal growth factor receptor-transforming growth factor. They tested this effect in three cell lines of lung adenocarcinoma, colon cancer, and breast cancer.

Evaluation of the influence of some gene expressions on anti-tumor drug cytotoxicity by Wang and coworkers provided the mechanism effect of connexin 43 as a tumor suppressor gene [96]. They used an SPR sensor to determine the influence of connexin 43 expressions on cisplatin cytotoxicity in different cancer cell lines. Their results exhibited that the SPR response curves had two stages. They showed that the changes which were related to connexin 43 expression in the first hour were interpreted by the SPR responses. In the second stage, the SPR response slowly decreased that was related to apoptosis. They compared the SPR measurements from several conventional biological assays with their system, and the results showed that cellular response to cisplatin in the period of oxidative stress could be affected by the connexin 43 expression.

Sari et al. developed an SPR sensor to determine erythromycin in the aqueous solution [97]. They combined the three techniques that were mini-emulsion polymerization, molecular imprinting, and SPR. They obtained R^2 and LOD values as 0.99 and 0.29 ppm, respectively. They also determined the selectivity property of this SPR sensor by using kanamycin sulfate, neomycin sulfate, and spiramycin. They claimed that the SPR sensor had low cost, was rapid, and provided reliable results in order to be used in the detection of erythromycin from aqueous solution.

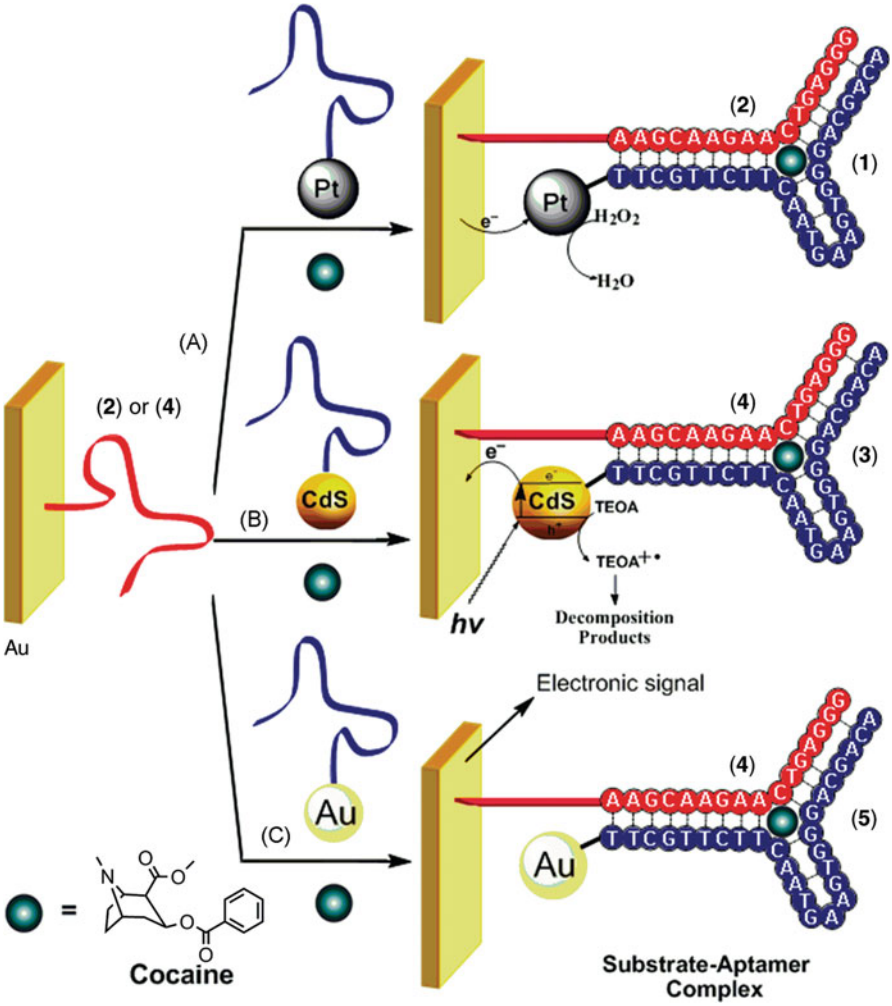

Fig. 10.16 (**a**) Electrochemical, (**b**) photoelectrochemical, and (**c**) SPR analysis [94]

6 Conclusions and Future Perspectives

Up to now, more than 40,000 publications related to SPR sensors were reported by ISI Web of Knowledge. When the assignment of the topics was analyzed, the impacts of the technologies were critically on medical diagnosis. Recently, the researchers demonstrated that the several studies on applications of real samples has performed.

In this chapter, different kinds of platforms and emerging technological inventions like coupling between SPR system and nanoparticles, microfluidics, or designing chips, analytical performance improvements for clinical diagnosis were

considered. As a case study, hormones detection associated with the endocrine disorders, protein biomarkers in relation to cancer and cardiac diseases, and immune system disease diagnoses by antibody detection were discussed. In addition, nucleic acid sensing was reviewed for genetic disorders and pathogens detections. Finally, immunosensing approaches were discussed for pathogens detection.

Innovative surface chemistry development and antifouling strategies guarantee decreased non-specific binding, which is necessary for biological fluids analysis with reduced sample pretreatment, dilution, heat, or filtration. In summary, SPR sensors propose comparable analytical performances to conventional methods used in medical diagnosis by ensuring real-time monitoring, label-free detection, parallel analysis, high-throughput analysis, little sample pretreatment, fast responses, and low cost. Considering these reasons, it is believed, in the near future, SPR will appear as an efficient, powerful, and alternative system for daily routine clinical analysis by opening also new horizons for future developments in personalized medicine and in point-of-care diagnostics. So far, published information originated from academic studies and the application of SPR sensors for medical diagnosis will obtain momentum in the next future.

References

1. Labib M, Sargent EH, Kelley SO (2016) Electrochemical methods for the analysis of clinically relevant biomolecules. Chem Rev 116:9001–9090
2. Stojanović I, Schasfoort RBM, Terstappen LWMM (2014) Analysis of cell surface antigens by surface plasmon resonance imaging. Biosens Bioelectron 52:36–43
3. Saylan Y, Yılmaz F, Derazshamshir A, Yılmaz E, Denizli A (2017) Synthesis of hydrophobic nanoparticles for real-time lysozyme detection using surface plasmon resonance sensor. J Mol Recognit 30:e2631.1–7
4. Saylan Y, Akgönüllü S, Çimen D, Derazshamshir A, Bereli N, Yılmaz F, Denizli A (2017) Surface plasmon resonance nanosensors based on molecularly imprinted nanofilm for detection of pesticides. Sensors Actuators B Chem 241:446–454
5. Ronkainen NJ, Halsall HB, Heineman WR (2010) Electrochemical biosensors. Chem Soc Rev 39:1747–1763
6. Guerreiro GV, Zaitouna AJ, Lai RY (2014) Characterization of an electrochemical mercury sensor using alternating current, cyclic, square wave and differential pulse voltammetry. Anal Chim Acta 810:79–85
7. Campuzanoa S, Kuralay F, Lobo-Castañón MJ, Bartošík M, Vyavaharea K, Paleček E, Haake DA, Wang J (2011) Ternary monolayers as DNA recognition interfaces for direct and sensitive electrochemical detection in untreated clinical samples. Biosens Bioelectron 26(8):3577–3583
8. Atay S, Pişkin K, Yılmaz F, Çakır C, Yavuz H, Denizli A (2016) Quartz crystal microbalance based biosensors for detecting highly metastatic breast cancer cells via their transferrin receptors. Anal Methods 8:153–161
9. Çiçek Ç, Yılmaz F, Özgür E, Yavuz H, Denizli A (2016) Molecularly imprinted quartz crystal microbalance sensor (QCM) for bilirubin detection. Chemosensors 4(4):21–34
10. Sener G, Ozgur E, Yılmaz E, Uzun L, Say R, Denizli A (2010) Quartz crystal microbalance based nanosensor for lysozyme detection with lysozyme imprinted nanoparticles. Biosens Bioelectron 26:815–821
11. Wang Y, Li J, Viehland D (2014) Magnetoelectrics for magnetic sensor applications: status, challenges and perspectives. Mater Today 17(6):269–275

12. Melzer M, Karnaushenko D, Lin G, Baunack S, Makarov D, Schmidt OG (2015) Direct transfer of magnetic sensor devices to elastomeric supports for stretchable electronics. Adv Mater 27(8):1333–1338
13. Zhang Y, Shen J, Yang H, Yang Y, Zhou Z, Yang S (2015) A highly selective magnetic sensor for Cd^{2+} in living cells with (Zn, Mn)-doped iron oxide nanoparticles. Sensors Actuators B Chem 207:887–892
14. Peiker P, Oesterschulze E (2015) Geometrically tuned wettability of dynamic micromechanical sensors for an improved in-liquid operation. Appl Phys Lett 107(10):101903–101907
15. Borin D, Melli M, Zilio SD, Toffoli V, Scoles G, Toffoli G, Lazzarino M (2014) How to engineer superhydrophobic micromechanical sensors preserving mass resolution. Sensors Actuators B Chem 199:62–69
16. Hu KM, Zhang WM, Shi X, Yan H, Peng ZK, Meng G (2016) Adsorption-induced surface effects on the dynamical characteristics of micromechanical resonant sensors for in situ real-time detection. J Appl Mech 83(8):081009–081020
17. Guo X (2012) Surface plasmon resonance based biosensor technique: a review. J Biophotonics 5(7):483–501
18. Fu E, Chinowsky T, Nelson K, Yager P (2008) Chapter 10: SPR imaging for clinical diagnostics. In: Handbook of surface plasmon resonance. Royal Society of Chemistry, Cambridge, pp 313–332
19. Caucheteur C, Guo T, Albert J (2015) Review of plasmonic fiber optic biochemical sensors: improving the limit of detection. Anal Bioanal Chem 407:3883–3897
20. Wood RW (1902) On a remarkable case of uneven distribution of light in a diffraction grating spectrum. Philos Mag 4:396–402
21. Cowan JJ (1972) The surface plasmon resonance effect in holography. Opt Commun 5:69–72
22. Schneider FW (1982) Non-linear Raman spectroscopy and its chemical applications. Biological applications of resonance CARS, Reidel Publishing Company Dordrecht: Holland/Boston: USA/London: England vol 93, pp 445–459
23. Rothenbausler B, Knoll W (1988) Surface–plasmon microscopy. Nature 332:615–617
24. Hickel W, Knoll W (1989) Surface plasmon microscopic imaging of ultrathin metal coatings. Acta Metall 37:2141–2144
25. Otto A (1968) Excitation of nonradiative surface plasma waves in silver by the method of frustrated total reflection. Z Phys 16:398–410
26. Buck RP (1990) Biosensor technology: fundamentals and applications. Marcel Dekker, New York
27. Szentirmay Z (1992) Surface plasmon spectroscopy of metal/dielectric structures. Spectrochim Acta 48:9–17
28. Welford K (1991) Surface plasmon-polaritons and their uses. Opt Quant Electron 23:1–27
29. Gutiérrez-Gallego R, Llop E, Bosch J, Segura J (2011) Surface plasmon resonance in doping analysis. Anal Bioanal Chem 401:389–403
30. Masson JF (2017) Surface plasmon resonance clinical biosensors for medical diagnostics. ACS Sens 2(1):16–30
31. Situ C, Mooney MH, Elliott CT, Buijs J (2010) Advances in surface plasmon resonance biosensor technology towards high-throughput, food-safety analysis. TrAC Trends Anal Chem 29:1305–1315
32. Helmerhorst E, Chandler DJ, Nussio M, Mamotte CD (2012) Real-time and label-free bio-sensing of molecular interactions by surface plasmon resonance: a laboratory medicine perspective. Clin Biochem Rev 33:161–173
33. Tokel O, Yildiz UH, Inci F, Durmus NG, Ekiz OO, Turker B, Cetin C, Rao S, Sridhar K, Natarajan N, Shafiee H, Dana A, Demirci U (2015) Portable microfluidic integrated plasmonic platform for pathogen detection. Sci Rep 5:9152–9161
34. Laocharoensuk R (2016) Development of electrochemical immunosensors towards point-of-care cancer diagnostics: clinically relevant studies. Electroanalysis 28:1716–1729
35. Ouellet E, Lund L, Lagally E (2013) Chapter 30: Multiplexed surface plasmon resonance imaging for protein biomarker analysis. In: Microfluidic diagnostics. Methods in molecular biology, Springer Science+Business Media, LLC, Berlin/Heidelberg, Germany vol 949. pp 473–490

36. Kirsch J, Siltanen C, Zhou Q, Revzin A, Simonian A (2013) Biosensor technology: recent advances in threat agent detection and medicine. Chem Soc Rev 42:8733–8769
37. Ranjan R, Esimbekova EN, Kratasyuk VA (2017) Rapid biosensing tools for cancer biomarkers. Biosens Bioelectron 87:918–930
38. Aćimović SS, Ortega MA, Sanz V, Berthelot J, Garcia-Cordero JL, Renger J, Maerkl SJ, Kreuzer MP, Quidant R (2014) LSPR chip for parallel, rapid, and sensitive detection of cancer markers in serum. Nano Lett 14:2636–2641
39. Ertürk G, Özen H, Tümer MA, Mattiasson B, Denizli A (2016) Microcontact imprinting based surface plasmon resonance (SPR) biosensor for real-time and ultrasensitive detection of prostate specific antigen (PSA) from clinical samples. Sensors Actuators B Chem 224:823–832
40. Uludag Y, Tothill IE (2012) Cancer biomarker detection in serum samples using surface plasmon resonance and quartz crystal microbalance sensors with nanoparticle signal amplification. Anal Chem 84:5898–5904
41. Türkoğlu EA, Yavuz H, Uzun L, Akgöl S, Denizli A (2013) The fabrication of nanosensor-based surface plasmon resonance for IgG detection. Artif Cells Nanomed Biotechnol 41:213–221
42. Ertürk G, Uzun L, Tümer MA, Say R, Denizli A (2011) Fab fragments imprinted SPR biosensor for real-time human immunoglobulin G detection. Biosens Bioelectron 28(1):97–104
43. Dibekkaya H, Saylan Y, Yılmaz F, Derazshamshir A, Denizli A (2016) Surface plasmon resonance sensors for real-time detection of cyclic citrullinated peptide antibodies. J Macromol Sci, Part A: Pure Appl Chem 53:585–594
44. Chung JW, Kim SD, Bernhardt R, Pyun JC (2005) Application of SPR biosensor for medical diagnostics of human hepatitis B virus (hHBV). Sensors Actuators B Chem 111(112):416–422
45. Uzun L, Say R, Ünal S, Denizli A (2009) Production of surface plasmon resonance based assay kit for hepatitis diagnosis. Biosens Bioelectron 24:2878–2884
46. Lu J, Stappen TV, Spasic D, Delport F, Vermeire S, Gils A, Lammertyn J (2016) Fiber optic-SPR platform for fast and sensitive infliximab detection in serum of inflammatory bowel disease patients. Biosens Bioelectron 79:173–179
47. Ramanaviciene A, German N, Kausaite-Minkstimiene A, Voronovic J, Kirlyte J, Ramanavicius A (2012) Electrochemical and electroassisted chemiluminescence methods based immunosensor for the determination of antibodies against human growth hormone were performed as comparative studies by surface plasmon resonance. Biosens Bioelectron 36:48–55
48. Im H, Shao H, Park YI, Peterson VM, Castro CM, Weissleder R, Lee H (2014) Label-free detection and molecular profiling of exosomes with a nanoplasmonic sensor. Nat Biotechnol 32(5):490–495
49. He L, Pagneux Q, Larroulet I, Serrano AY, Pesquera A, Zurutuza A, Mandler D, Boukherroub R, Szunerits S (2017) Label-free femtomolar cancer biomarker detection in human serum using graphene-coated surface plasmon resonance chips. Biosens Bioelectron 89:606–611
50. Liang RP, Yao GH, Fan LX, Qiu JD (2012) Magnetic Fe3O4@Au composite-enhanced surface plasmon resonance for ultrasensitive detection of magnetic nanoparticle-enriched α-fetoprotein. Anal Chim Acta 737:22–28
51. Osman B, Uzun L, Beşirli N, Denizli A (2013) Microcontact imprinted surface plasmon resonance sensor for myoglobin detection. Mater Sci Eng C 33:3609–3614
52. Sener G, Uzun L, Say R, Denizli A (2011) Use of molecular imprinted nanoparticles as biorecognition element on surface plasmon resonance sensor. Sensors Actuators B Chem 160:791–799
53. Bocková M, Song XC, Gedeonová E, Levová K, Kalousová M, Zima T, Homola J (2016) Surface plasmon resonance biosensor for detection of pregnancy associated plasma protein A2 in clinical samples. Anal Bioanal Chem 408(26):7265–7269
54. Murakami K, Tokuda M, Suzuki T, Irie Y, Hanaki M, Izuo N, Monobe Y, Akagi K-i, Ishii R, Tatebe H, Tokuda T, Maeda M, Kume T, Shimizu T, Irie K (2016) Monoclonal antibody with conformational specificity for a toxic conformer of amyloid β42 and its application toward the Alzheimer's disease diagnosis. Sci Rep 6:29038–29050

55. Sankiewicz A, Romanowicz L, Laudanski P, Zelazowska-Rutkowska B, Puzan B, Cylwik B, Gorodkiewicz E (2016) SPR imaging biosensor for determination of laminin-5 as a potential cancer marker in biological material. Anal Bioanal Chem 408:5269–5276
56. Brun APL, Soliakov A, Shah DSH, Holt SA, McGill A, Lakey JH (2015) Engineered self-assembling monolayers for label free detection of influenza nucleoprotein. Biomed Microdevices 17:49–59
57. Liu Y, Liu Q, Chen S, Cheng F, Wang H, Peng W (2015) Surface plasmon resonance biosensor based on smart phone platforms. Sci Rep 5:12864–12873
58. Sener G, Ozgur E, Rad AY, Uzun L, Say R, Denizli A (2013) Rapid real-time detection of procalcitonin using a microcontact imprinted surface plasmon resonance biosensor. Analyst 138:422–428
59. Mariani S, Minunni M (2014) Surface plasmon resonance applications in clinical analysis. Anal Bioanal Chem 406:2303–2323
60. Cenci L, Andreetto E, Vestri A, Bovi M, Barozzi M, Iacob E, Busato M, Castagna A, Girelli D, Bossi AM (2015) Surface plasmon resonance based on molecularly imprinted nanoparticles for the picomolar detection of the iron regulating hormone Hepcidin-25. J Nanobiotechnol 13:51–66
61. Zhang Q, Jing L, Zhang J, Ren Y, Wang Y, Wang Y, Wei T, Liedberg B (2014) Surface plasmon resonance sensor for femtomolar detection of testosterone with water-compatible macroporous molecularly imprinted film. Anal Biochem 463:7–14
62. Vashist SK, Marion Schneider E, Barth E, Luong JHT (2016) Surface plasmon resonance-based immunoassay for procalcitonin. Anal Chim Acta 938:129–136
63. Treviño J, Calle A, Rodríguez-Frade JM, Mellado M, Lechuga LM (2009) Single- and multi-analyte determination of gonadotropic hormones in urine by surface plasmon resonance immunoassay. Anal Chim Acta 647:202–209
64. Treviño J, Calle A, Rodríguez-Frade JM, Mellado M, Lechuga LM (2009) Surface plasmon resonance immunoassay analysis of pituitary hormones in urine and serum samples. Clin Chim Acta 403:56–62
65. Srivastava SK, Verma R, Gupta BD, Khalaila I, Abdulhalim I (2015) SPR based fiber optic sensor for the detection of vitellogenin: an endocrine disruption biomarker in aquatic environments. Biosens J 4:1–5
66. Yockell-Lelièvre H, Bukar N, McKeating KS, Arnaud M, Cosin P, Guo Y, Dupret-Carruel J, Mouginb B, Masson JF (2015) Plasmonic sensors for the competitive detection of testosterone. Analyst 140:5105–5112
67. Sanghera N, Anderson A, Nuar N, Xie C, Mitchell D, Klein-Seetharaman J (2017) Insulin biosensor development: a case study. Int J Parallel Emergent Distrib Syst 32(1):119–138
68. Sharon E, Freeman R, Riskin M, Gil N, Tzfati Y, Willner I (2010) Optical, electrical and surface plasmon resonance methods for detecting telomerase activity. Anal Chem 82:8390–8397
69. Diltemiz SE, Denizli A, Ersöz A, Say R (2008) Molecularly imprinted ligand-exchange recognition assay of DNA by SPR system using guanosine and guanine recognition sites of DNA. Sensors Actuators B Chem 133:484–488
70. Bini A, Mascini M, Mascini M, Turner APF (2011) Selection of thrombin-binding aptamers by using computational approach for aptasensor application. Biosens Bioelectron 26:4411–4416
71. Kaur G, Paliwal A, Tomar M, Gupta V (2016) Detection of Neisseria meningitidis using surface plasmon resonance based DNA biosensor. Biosens Bioelectron 78:106–110
72. Gifford LK, Sendroiu IE, Corn RM, Luptak A (2010) Attomole detection of mesophilic DNA polymerase products by nanoparticle-enhanced surface plasmon resonance imaging on glassified gold surfaces. J Am Chem Soc 132:9265–9267
73. D'Agata R, Breveglieri G, Zanoli LM, Borgatti M, Spoto G, Gambari R (2011) Direct detection of point mutations in nonamplified human genomic DNA. Anal Chem 83:8711–8717
74. Cho H, Yeh EC, Sinha R, Laurence T, Bearinger J, Lee L (2012) Single-step nanoplasmonic VEGF165 aptasensor for early cancer diagnosis. ACS Nano 6:7607–7614

75. Jahanshahi P, Zalnezhad E, Sekaran SD, Adikan FRM (2014) Rapid immunoglobulin M-based dengue diagnostic test using surface plasmon resonance biosensor. Sci Rep 4:3851–3858
76. Altintas Z, Pocock J, Thompson KA, Tothill IE (2015) Comparative investigations for adenovirus recognition and quantification: plastic or natural antibodies? Biosens Bioelectron 74:996–1004
77. Basso CR, Tozato CC, Ribeiro MCM, Junior JPA, Pedros VA (2013) A immunosensor for the diagnosis of canine distemper virus infection using SPR and EIS. Anal Methods 5:5089–5096
78. Bai H, Wang R, Hargis B, Lu H, Li Y (2012) A SPR aptasensor for detection of avian influenza virus H5N1. Sensors 12:12506–12518
79. Diltemiz SE, Ersöz A, Hür D, Keçili R, Say R (2013) 4-Aminophenyl boronic acid modified gold platforms for influenza diagnosis. Mater Sci Eng C 33:824–830
80. Altintas Z, Gittens M, Guerreiro A, Thompson KA, Walker J, Piletsky S, Tothill IE (2015) Detection of waterborne viruses using high affinity molecularly imprinted polymers. Anal Chem 87:6801–6807
81. Riedel T, Rodriguez-Emmenegger C, Santos Pereira A, Bědajánková A, Jinoch P, Boltovets PM, Brynda E (2014) Diagnosis of Epstein–Barr virus infection in clinical serum samples by an SPR biosensor assay. Biosens Bioelectron 55:278–284
82. Yilmaz E, Majidi D, Ozgur E, Denizli A (2015) Whole cell imprinting based Escherichia Coli sensors: a study for SPR and QCM. Sensors Actuators B Chem 209:714–721
83. Wang Y, Ye Z, Si C, Ying Y (2011) Subtractive inhibition assay for the detection of E. coli O157:H7 using surface plasmon resonance. Sensors 11:2728–2739
84. Karoonuthaisiri N, Charlermroj R, Morton MJ, Oplatowska-Stachowiak M, Grant IR, Elliott CT (2014) Development of a M13 bacteriophage-based SPR detection using Salmonella as a case study. Sensors Actuators B Chem 190:214–220
85. Arya SK, Singh A, Naidoo R, Wu P, McDermott MT, Evoy S (2011) Chemically immobilized T4-bacteriophage for specific Escherichia coli detection using surface plasmon resonance. Analyst 136:486–492
86. Kuo YC, Ho JH, Yen TJ, Chen HF, Lee OKS (2011) Development of a surface plasmon resonance biosensor for real-time detection of osteogenic differentiation in live mesenchymal stem cells. PLoS One 6(7):e22382–e22389
87. Yanase Y, Hiragun T, Yanase T, Kawaguchi T, Ishii K, Hide M (2013) Application of SPR imaging sensor for detection of individual living cell reactions and clinical diagnosis of type I allergy. Allergol Int 62:163–169
88. Yanase Y, Hiragun T, Yanase T, Kawaguchi T, Ishii K, Kumazaki N, Obara T, Hide M (2014) Clinical diagnosis of type I allergy by means of SPR imaging with less than a microliter of peripheral blood. Sens Bio-Sens Res 2:43–48
89. Altintas Z, France B, Ortiz JO, Tothill IE (2016) Computationally modelled receptors for drug monitoring using an optical based biomimetic SPR sensor. Sensors Actuators B Chem 224:726–737
90. Altintas Z, Guerreiro A, Piletsky SA, Tothill IE (2015) NanoMIP based optical sensor for pharmaceuticals monitoring. Sensors Actuators B Chem 213:305–313
91. Yockell-Lelièvre H, Bukar N, Toulouse JL, Pelletiera JN, Masson JF (2016) Naked-eye nanobiosensor for therapeutic drug monitoring of methotrexate. Analyst 141:697–703
92. Pernites RB, Ponnapati RR, Felipe MJ, Advincula RC (2011) Electropolymerization molecularly imprinted polymer (E-MIP) SPR sensing of drug molecules: pre-polymerization complexed terthiophene and carbazole electroactive monomers. Biosens Bioelectron 26:2766–2771
93. Pernites RB, Ponnapati RR, Advincula RC (2010) Surface plasmon resonance (SPR) detection of theophylline via electropolymerized molecularly imprinted polythiophenes. Macromolecules 43:9724–9735

94. Golub E, Pelossof G, Freeman R, Zhang H, Willner I (2009) Electrochemical, photoelectrochemical, and surface plasmon resonance detection of cocaine using supramolecular aptamer complexes and metallic or semiconductor nanoparticles. Anal Chem 81:9291–9298
95. Wang Y, Zhang C, Zhang Y, Fang H, Min C, Zhu S, Yuan XC (2015) Investigation of phase SPR biosensor for efficient targeted drug screening with high sensitivity and stability. Sensors Actuators B Chem 209:313–322
96. Wang Y, Zhang S, Zhang C, Zhao Z, Zheng X, Xue L, Liu J, Yuan XC (2016) Investigation of an SPR biosensor for determining the influence of connexin 43 expression on the cytotoxicity of cisplatin. Analyst 141:3411–3421
97. Sari E, Üzek R, Duman M, Denizli A (2016) Fabrication of surface plasmon resonance nanosensor for the selective determination of erythromycin via molecular imprinted nanoparticles. Talanta 150:607–614